Intermediate Filaments Formed De Novo from Tail-less Cytokeratins in the Cytoplasm and in the Nucleus

Bernhard L. Bader, Thomas M. Magin, Martina Freudenmann, Sabine Stumpp, and Werner W. Franke

Institute of Cell and Tumor Biology, German Cancer Research Center, D-6900 Heidelberg, Germany

Abstract. The roles of the different molecular domains of intermediate filament (IF) proteins in the assembly and higher order organization of IF structures have recently been studied by various groups but with partially controversial results. To examine the requirement of the aminoterminal (head) and the carboxyterminal (tail) domain of cytokeratins (CKs) for de novo IF formation in the living cell, we have constructed cDNAs coding for intact as well as head- and/or tail-less human CKs 8 and 18 and the naturally tail-less human CK 19, all under the control of the human β-actin promoter. After transient and stable transfections of mouse 3T3-L1 cells, which are devoid of any CKs, we have studied, with such constructs, the resulting gene products by gel electrophoresis and immunolocalization techniques. By light and electron microscopy we show that extended cytoplasmic IF meshworks are formed from pairs of the type II CK 8 with the type I CKs 18 or 19 as well as from pairs of tail-less CK 8 with tail-less CKs 18 or 19 in the transfected cells, proving that the absence of the tail domain in both types of CKs does not prevent the de novo formation of regular IFs. Most surprisingly, however, we have observed spectacular alterations in the nucleocytoplasmic distribution of the IFs formed from tail-less CKs. In many of the transfected cells, a large part, or all, of the detectable CKs was found to occur in extensive IF bundles in the nucleoplasm. Intranuclear accumulations of CK deposits, however mostly nonfibrillar, were also observed when the cells had been transfected with cDNAs encoding tail-less CKs also lacking their head domains, whereas CKs deleted only in the head domain were found exclusively in the cytoplasm. The specific domain requirements for the assembly of cytoplasmic IF bundles are discussed and possible mechanisms of intranuclear accumulation of IFs are proposed.

INTERMEDIATE filaments (IFs)[1] are cell type-specific prominent protein polymer structures of most vertebrate cells (for example see references 16, 23, 69), represented by a large multigene family. IF proteins form filamentous structures restricted to the cytoplasm, except for one subgroup, the lamins (A and B type), which accumulate in the cell nucleus and form the nuclear lamina, their specific topogenesis being controlled by a nuclear migration motif (for review see reference 54). IF polypeptides display a common structural principle: a central α-helical rod domain of relatively well-conserved length ($\sim$310 amino acid residues in the case of cytoplasmic IFs) is flanked by a head and a tail domain which can vary between different IF proteins in length and in amino acid sequence. While the assembled rods form the typical protofilament backbone structure with a tetrameric (two coiled-coils) subunit, the head and tail domains are thought not to be part of the filamentous backbone but to protrude laterally and contribute to protofilament and IF packing, and to IF interaction with other cellular components (1, 7, 36, 69-71).

Among the IF proteins, the cytokeratins (CKs) represent the most complex subgroup of IF proteins, comprising in the human genome at least 20 different epithelial (55, 56) and 10 trichocytic (hair-type; reference 35) genes. CKs fall into two subclasses, type I and II polypeptides, which share only $\sim$30% amino acid sequence homology, concentrated in the rod portion (23). In contrast to the other IF proteins which can assemble into homopolymeric IFs in vitro and in vivo, CK IFs are obligatory heteropolymers in that at least one polypeptide from either CK subclass is required to form stable subunits and IFs (cf. references 10, 11, 23, 32, 40, 45, 69, 76).

Studies, in vitro and in vivo, of the possible contributions of the head and/or tail domains to IF formation are considerably controversial. In such studies the requirements and contributions of the specific protein domains and sequence elements have been examined after removal of the head and/or tail domain by proteases or in deletion mutations. The mutated protein was then either produced in *Escherichia coli*, for in vitro studies, or was expressed in cells that had been transfected with an appropriate cDNA-derived construct or injected with mRNA obtained by transcription in vitro. In such experiments, most of the head domain appears important for IF formation. Specifically, several groups have concluded that most of the head domain has to be present for

1. *Abbreviations used in this paper*: CK, cytokeratin; IF, intermediate filament; and NF, neurofilament.

an assembly to homopolymeric IF structures (desmin: see references 26, 39, 62, 74; vimentin: see reference 72; glial fibrillary protein: see reference 61), whereas dimeric or tetrameric subunits can still be formed from such truncated proteins (for example see references 39, 61). Isolated head portions of desmin have been reported also to dimerize but, of course, do not form filaments (for example see reference 63).

Different results, however, have been published as to the requirements of tail sequences. Kaufmann et al. (39) as well as Shoeman et al. (65) have reported that proteolytic removal of major portions from desmin or vimentin does not significantly reduce the capability to form typical IFs, whereas Quinlan et al. (61) have described that a cDNA-derived glial fibrillary protein molecule practically lacking the entire tail was not able to form IFs. Using a different approach, Birkenberger and Ip (7) have noticed that the presence of a synthetic nonapeptide representing a tail sequence during assembly in vitro results in IFs with a markedly looser protofilament packing, which these authors took as an indication of a contribution of tail sequences to higher order IF arrangement.

The situation with CKs is especially complicated due to the fact that they can only form IFs as heteropolymers of type I and II polypeptides. Here, the heterophilic interaction is clearly located in the rod, apparently at multiple sites, as CK molecules representing only the rod domain, or part of it, recognize polypeptides of the complementary subfamily with high avidity and specificity, and form stoichiometric type I:type II oligomers but not IFs (8, 34, 52; for review see reference 69).

The existence of a practically tail-less type I CK, i.e., CK 19, in naturally occurring IFs, together with one type II CK partner, shows that a tail domain is not categorically required (5, 6, 68). Head- and/or tail-deletion mutants of CK 14 (type I) molecules can co-polymerize with endogenous type II CKs and integrate into a pre-existing IF fibril system, and these mutant molecules can also assemble with intact CK 5 into IFs in vitro (2, 3, 8). However, conclusions from such observations as to tail functions are limited as the tail of one subclass partner in the CK heterooligomer subunit may be sufficient. Therefore, Hatzfeld and Weber (33) have combined the tail-deleted CK 8 (type II) with the naturally tail-less CK 19 in vitro and found assembly into normal-looking IFs. In contrast, Lu and Lane (51) have emphasized that in vivo, upon transfection of mouse NIH 3T3 cells lacking CKs with various deletion cDNAs, at least one intact CK polypeptide, i.e., one tail domain of either a type I or a type II CK in the heterotypic complex, is necessary for producing extensive IF meshworks. These authors have also reported that the combination of tail-clipped CK 8 (2/3 removed) with naturally tail-less CK 19 or with a tail-deletion mutant of CK 18 interferes with the formation of CK fibril meshworks.

We have been studying over the past decade the structures formed by CKs introduced into various kinds of epithelial and nonepithelial cells by either RNA microinjection or DNA transfection, examining the integration into pre-existing CK IF bundles or filament formation de novo (for example see references 17, 43, 53). Here we report our results of transfection experiments using intact as well as head- and/or tail-deleted cDNA constructs for CKs 8, 18, and 19 in transient and stable transfectants. We show that the naturally tail-less human CK 19 as well as a tail-less deletion mutant of CK 18 are able, in combination with a tail-less CK 8, to assemble into extensive arrays of IFs. Unexpectedly, we have noted in such experiments that for the tail-less mutants the normal compartmentalization can be lost, resulting in an accumulation of these mutants in the nucleus where they form typical IF bundles.

Materials and Methods

Cloning of Complete and Truncated Cytokeratin cDNAs

In our study the following cDNAs were used. (*a*) Cloning of cDNA coding for the entire human CK 8 has been described (53). (*b*) For the construction of a cDNA clone of the complete human CK 19, the Nar I/Kpn I fragment of 426 bp of the subclone pH19/XS 5.5 containing most of exon 1, derived from the genomic phage clone λH 19/8 was ligated to the unique Kpn I site of the cDNA clone pcH19/6.1 (6). (*c*) Clone pHK18-P-7 representing a cDNA of the complete human CK 18 was generated by complementing the cDNA of the plasmid pKH 18^1 (49) with a CK 18 cDNA fragment obtained by polymerase chain reaction (PCR; 22, 47, 53). (*d*) The cDNA coding for tail-less human CK 8 (CK 8ΔT) was synthesized by PCR, using the CK 8 cDNA pHK 8-P5 (53) as template, the 5′-amplimer P1 (5′-d[GTAAAACGACGGCCAGT]-3′, M13 primer; Pharmacia, Freiburg, Germany), and the 3′-amplimer P2 (5′-d[CGGCGCGGATCCTTACAGCCGGCTCTCCTCGCCCTC]-3′) as primers. (Bold letters of P2 correspond to nucleotides 574–594 of clone pHK 8^1; i.e., the sequence EGEESRL [see Fig. 1; cf. 49].) The 3′-amplimer P2 encodes a translation termination codon and a unique cloning site (see Fig. 1, *a* and *b*). (*e*) The cDNA coding for tail-less CK 18 (CK 18ΔT) was also synthesized by PCR (see Fig. 1, *a* and *c*), using as template the CK 18 cDNA pHK18-P7 and as primers the 5′-amplimer P1 together with the 3′-amplimer P3 (5′-d[GCCAAGCTTTTACTCGCCATCTTCCAGCAGGCG]-3′). Bold letters of P3 correspond to nucleotides 1126–1146; i.e., RLLEDGE (see Fig. 1; references 49, 60). (*f*) A head-deleted CK 8 mutant (CK ΔH8) starting at amino acid position 91 (42; i.e., with MEKEQIKT) was produced using the 5′-amplimer P4 (5′-d[ACCGCG*GTCGAC*CCACCATGGAGAAGGAGCAGATCAAGACC]-3′), corresponding to nucleotides 1383–1403 (42), and as 3′-amplimer the M13 reverse primer P5 (5′-d[CAGGAAACAGCTATGAC]-3′). (*g*) The double-truncated CK 8 mutant without head and tail domain (CK ΔH8ΔT) was produced by the combined use of the amplimers P2 (see *d*) and P4 (see *f*). (*h*) A head-deleted CK 18 (CK ΔH18) was obtained using 5′-amplimer P6 (5′-[GAC*GTCGAC*ACCATGCAAAGCCTGAACGACCGC]-3′; 49) and 3′-amplimer P5 (see *f*), so that the resulting polypeptide started at position 84 with MQSLNDR; i.e., corresponding to nucleotides 232–252 (cf. 49). (*i*) The double-deletion of CK 18 (CK ΔH18ΔT) was generated by the combined use of amplimers P3 (see construct described under *e*) and P6 (see construct described under *h*). (*j*) A head-deleted CK 19 (CK ΔH19) was produced from the cDNA clone described earlier (in *b*) in such a way that the resulting truncated polypeptide started at position 69 (6), i.e., with MLTASDG, first by a deletion of the sequence upstream of the Kpn I-site at nucleotide position 736 by Hind III/Kpn I-double digestion, followed by resynthesis of the complete 5′ untranslated region, up to the initiation codon, from an oligonucleotide fused in frame with a synthetic linker of four overlapping oligonucleotide pairs bridging nucleotides 592-736.

PCR was carried out with 100 ng of linearized plasmid as template, 25 mM dNTP, 250 ng of each amplimer, standard PCR reaction buffer (50 mM KCl, 10 mM Tris-HCl, pH 8, 1.5 mM $MgCl_2$, 0.01% BSA), 2.5 U AmpliTaq (Perkin-Elmer Cetus, Norwalk, CT) and cycle conditions as follows: denaturation at 92°C for 1 min, annealing at 56°C for 45 s, and synthesis at 72°C for 1 min for 30 cycles.

For cloning, DNA sequencing and in vitro transcription/translation studies the cDNAs were cloned into Bluescript and Bluescribe plasmids (Stratagene, La Jolla, CA). The DNA sequences of the final products were determined as described (53). The amino acid sequences of the COOH-termini of tail-less CKs 8 and 18 are described under CK 8ΔT and CK 18ΔT in Fig. 1. RNAs synthesized by transcription in vitro were processed for in vitro translation, and the products were analyzed by gel electrophoresis as described by Leube et al. (50). To generate CK "mini-genes", the various CK cDNAs were introduced into the mammalian expression plasmid "pHβ APr-1-neo" (31).

RNAs were detected by Northern blotting as described (6).

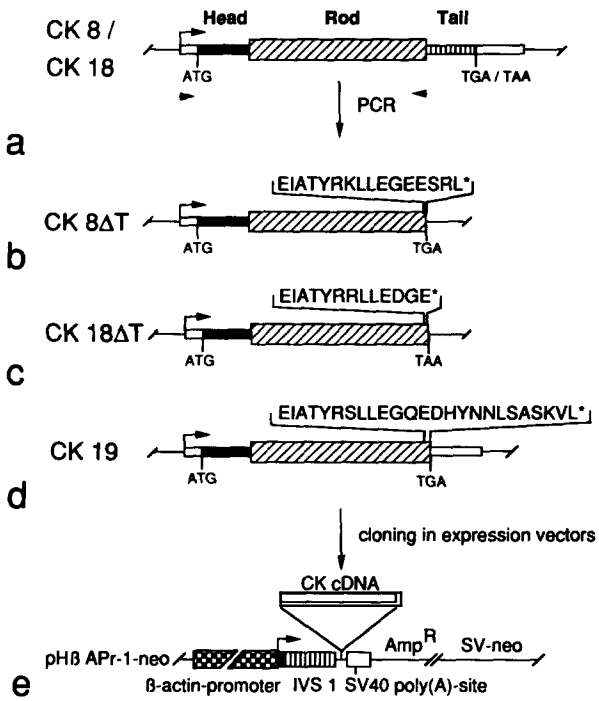

Figure 1. Schematic drawings showing the cloning strategy and the major cDNA constructs of intact and tail-less CKs used in this study. (*a*) Complete cDNAs representing the entire region coding either for CK 8 or CK 18. The three large domains are represented by a black bar (*Head*), thick hatched rectangle (*Rod*), and a striped bar (*Tail*). Open rectangles represent the 5'- and 3'-nontranslated regions. Direction of in vitro transcription by either T3 or T7 RNA polymerases in the plasmid vector Bluescript is indicated by the arrow. Translation initiation and termination codons are labeled *ATG* and *TGA/TAA*. Arrowheads indicate the positions of the 5'- and 3'-amplimer primers used for PCR (for tail-less CKs 8 and 18). (*b* and *c*) The cDNAs coding for tail-less CKs 8 (CK8ΔT) and 18 (CK 18ΔT) generated by PCR, using amplimers including a termination codon at the region corresponding to the end of the α-helical rod (*asterisk*). The resulting carboxyterminal amino acid sequences of CKs 8ΔT and 18ΔT are shown in one-letter code. (*d*) Complete cDNA of CK 19. Symbols as in *a–c*; the amino acid sequence of the natural carboxyterminal region is also shown. (*e*) To express the various CK cDNAs in eukaryotic cells they were cloned into appropriate linker sites of the expression vector pHβ APr-1-neo. The key regulatory elements of this plasmid are as follows: human β-actin gene promoter; IVS, intron 1 of the human β-actin gene; SV-40 polyadenylation site; Amp^R: β-lactamase gene; SVneo, neomycin resistance gene under the control of the SV40 early promoter.

Cell Culture, Transfection, and Protein Analyses

Murine 3T3-L1 cells (preadipocytes) obtained from Flow Laboratories, Inc. (Meckenheim, Germany) were kept in DME containing 10% FCS (30). Stable and transient cDNA transfections were carried out by the Ca^{2+}-phosphate technique (29). Cells of selected clones were grown first in the

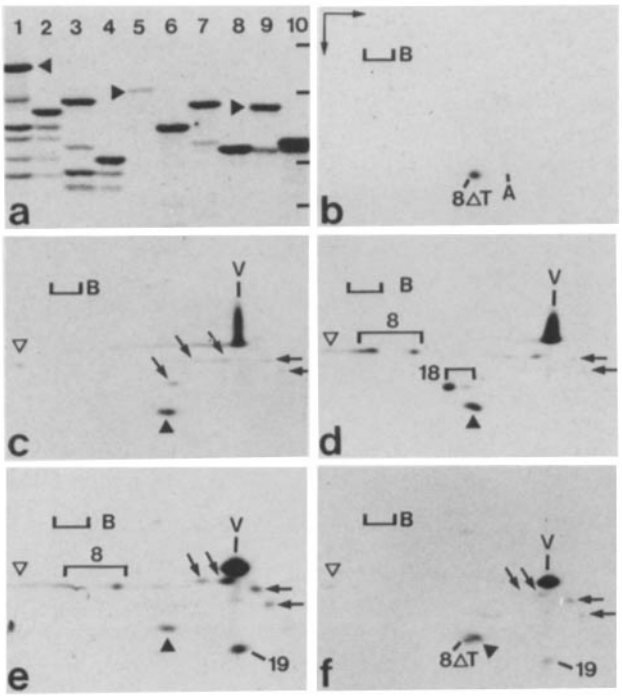

Figure 2. Analyses of in vitro translation products of cDNA constructs encoding intact and truncated CKs (*a* and *b*) and cytoskeletal proteins from untransfected (*c*) and transfected (*d–f*) 3T3-L1 cells, using SDS-PAGE (*a*) and two-dimensional gel electrophoresis, with IEF in the first (*upper left corner, horizontal arrow*) and SDS-PAGE in the second (*downward arrow*) dimension (*b–f*). (*a*) Fluorograph of [^{35}S]methionine-labeled polypeptides obtained by in vitro translation of in vitro synthesized RNAs coding for the intact CKs 8 (lane *1*), 18 (lane *5*), and 19 (lane *9*) (polypeptides indicated by *arrowheads*), for the tail-deleted CKs 8ΔT (lane *3*) and 18ΔT (lane *7*), for the head-less CKs ΔH8 (lane *2*) and ΔH18 (lane *6*), or the head- and tail-less CKs ΔH8ΔT (lane *4*), ΔH18ΔT (lane *8*), and ΔH19 (lane *10*). Bars on the right margin denote (from top to bottom) the positions of co-electrophoresed molecular weight markers such as BSA (66 kD), ovalbumin (45 kD), glyceraldehyde-3-phosphate dehydrogenase (36 kD), and carbonic anhydrase (29 kD). The carboxyterminal amino acid sequences of the CK tail truncations are as shown in Fig. 1. The aminoterminal amino acid sequences of the CK head truncations are as follows: CK ΔH8: MEKEQIKTLNNK...; CK ΔH18: MQSLNDRLASYL...; CK ΔH19: MLTASDGLLAG.... (*b*) Fluorograph of two-dimensional gel electrophoresis of [^{35}S]methionine-labeled in vitro translation product of tail-less CK 8ΔT(*8ΔT*) after co-electrophoresis with unlabeled reference proteins (positions indicated) rabbit α-actin (*A*) and BSA (*B*). (*c–f*) Co-electrophoreses of [^{35}S]methionine-labeled cytoskeletal proteins from untransfected 3T3-L1 cells (*c*), and 3T3-L1 cells transfected with various CK cDNA constructs coding for human CKs 8 and 18 (*d*), human CKs 8 and 19 (*e*), and the tail-less human CKs 8ΔT and 19 (*f*), with unlabeled IF proteins from human MCF-7 epithelial cells (cf. 6, 55), and reference proteins rabbit α-actin (*solid triangles*) and BSA (*B*). (*c*) Fluorograph of metabolically labeled cytoskeletal proteins of 3T3-L1 cells, with vimentin (*V*) as the only detectable IF protein and residual β- and γ-actin (*solid triangle*). *Short arrows*, typical degradation products of vimentin. The open triangle points to an as yet unknown cytoskeletal polypeptide. (*d*) Fluorograph of labeled IF proteins of a stably transfected 3T3-L1 cell line synthesizing murine vimentin (*V*) and human CKs 8 (*8*) and 18 (*18*). *Bracket*, position of the isoelectric variants. Symbols are as in *c*. (*e*) Fluorograph of labeled IF proteins from stably transfected 3T3-L1 cells synthesizing murine vimentin (*V*; *small arrows*, degradation products, as in *c*) and human CKs 8 (*8*) and 19 (*19*). Symbols are as in *c* and *d*. (*f*) Fluorograph of labeled IF proteins from stably transfected 3T3-L1 cells synthesizing vimentin (*V*) as well as tail-less human CKs 8ΔT (*8ΔT*) and 19 (*19*). Other symbols are as in *c*.

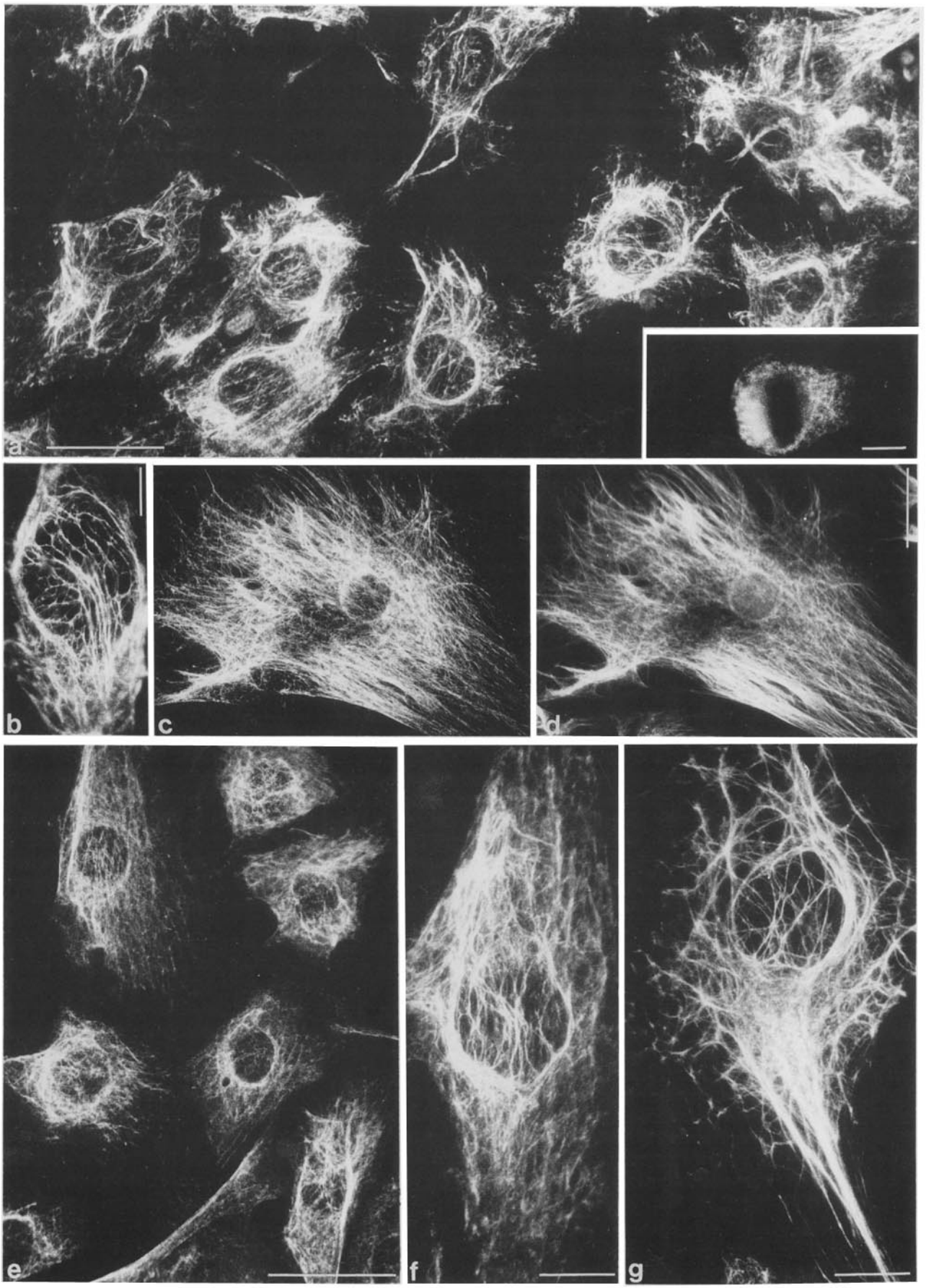
a
b
c
d
e
f
g

presence of 1 mg/ml G-418 (Gibco Laboratories, Karlsruhe, Germany) and later also without G-418. In some experiments cells were exposed to 10^{-6} M colcemid for 14 h. For in vivo labeling, cells were grown from 4–15 h in the presence of 200 μCi of [^{35}S]methionine (1,200 Ci/mMol; Amersham-Buchler, Braunschweig, Germany) in medium of reduced methionine content (40).

Preparation of cytoskeletal proteins as well as gel electrophoresis and polypeptide immunoblotting were as described (53).

Immunofluorescence and Electron Microscopy

Broad-range CK antibodies as well as antibodies specific for individual CKs or for a subset of CKs were used. Broad-range murine monoclonal such as IFA and CK antibodies lu-5 and K_G 1-8.136 (20, 40, 41, 52) and guinea pig antibodies reactive with CKs 8, 18, and/or 19 (provided by Dr. G. Bruder, Progen Biotechnics, Heidelberg, Germany) have been described (cf. 6, 40, 41). Human CK 8 was recognized by CK 8-specific monoclonal antibodies such as CAM 5.2, M20, and K_s8.17.2 (cf. 41). Human CK 18 was detected by monoclonal antibody K_s18.174.1 and CK 19 was detected by the monoclonal antibody K_s19.2-Z105 (Progen Biotechnics) or a specific rabbit antiserum (kindly provided by Dr. J. G. Rheinwald, Dana Farber Cancer Institute, Harvard Medical School, Boston, MA). Vimentin was recognized with specific guinea pig antibodies or murine mAb Vim 3B4 (Progen Biotechnics; Boehringer Mannheim GmbH, Mannheim, Germany; cf. 6). Murine as well as guinea pig antibodies to nuclear lamins were obtained from Dr. G. Krohne (Institute of Cell and Tumor Biology, German Cancer Research Center, Heidelberg, Germany). In addition, we used monoclonal antibodies to desmoplakins (DPI&2-2.15, 2.17, and 2.19), plakoglobin (PG 5.1), and desmoglein (DG 3.10; cf. 9, 21).

Basic procedures for light and electron microscopy have been described (6, 9). In most immunolocalization experiments at the electron microscopic level, the normal procedure was modified as follows. Cultured cells grown on coverslips were fixed with 2% formaldehyde in PBS (freshly made from paraformaldehyde) for 5 or 15 min, treated with 0.1% saponin in PBS for 15 min, or with 1% Triton in PBS (preferentially in studies of nuclear structures) for 3 min. Cells were washed with PBS and incubated with CK-specific antibodies for 1.5–2.0 h.

Results

Synthesis of Intact and Tail-less Human CKs In Vitro and in 3T3-L1 Cells Transfected with cDNA Constructs

For transfection studies, cDNAs coding for intact and head- and/or tail-truncated human CKs 8, 18, and 19 were inserted first into the bacterial plasmid Bluescript and then into the mammalian expression plasmid pHβ APr-1-neo to generate CK mini-genes (Fig. 1). To verify the nature of the encoded proteins we synthesized sense-RNA by transcription in vitro with T3 or T7 RNA polymerase from linearized CK cDNA Bluescript constructs and identified the corresponding products by in vitro translation, using [^{35}S]methionine labeling and gel electrophoresis (Fig. 2, *a* and *b*).

Mouse 3T3-L1 cells were used as host cells to study the domain requirements for de novo filament formation of human CKs 8, 18, and 19 because, in extensive examinations (18, 40, 41), these cells have never been noted spontaneously to synthesize CKs; endogenous CKs were neither induced nor stabilized after cDNA transfection with cDNAs encoding either type I or type II CKs (data not shown), in contrast to observations made with certain sublines of NIH 3T3 cells (28, 48; see also references 11, 45, 51). In the present study, identical results were obtained with cells transiently transfected and with stably transfected and selected cell clones as well as after microinjection of mRNA synthesized in vitro from the same cDNA constructs (not shown). "Negative cells," i.e., cells without any positive CK immunofluorescence, were not only seen upon transient transfections, but also in stably transfected cell clones, where they occurred at variable, sometimes high frequencies, probably reflecting the results of negative control mechanisms of an as yet unknown nature (for similar observations see also reference 45).

Untransfected 3T3-L1 cells and G-418-resistant 3T3-L1 cell clones stably transfected with one kind or combinations of mini-genes coding for human CKs, were examined for the presence of CKs by biochemical analyses of cytoskeletal proteins (Fig. 2, *c–f*) and by immunofluorescence microscopy (Figs. 3–7). The CKs present in the different cell clones were biochemically identified either by metabolic labeling with [^{35}S]methionine, followed by two-dimensional gel co-electrophoresis with the authentic cytoskeletal proteins, or by immunoblotting of electrophoretically separated proteins with different CK antibodies.

When IF proteins from untransfected radioactively labeled 3T3-L1 cells were examined by fluorography (Fig. 2 *c*) or immunoblotting using antibody IFA (not shown), the only IF protein detected was vimentin. In cells double transfected with the cDNA constructs coding for intact CKs 8 and 18 (Fig. 2 *d*) or CKs 8 and 19 (Fig. 2 *e*) two additional spots were seen. Labeled CKs 8 and 18 (Fig. 2 *d*) or CKs 8 and 19 (Fig. 2 *e*) comigrated with the authentic unlabeled human CKs 8, 18, and 19 (Fig. 2, *d* and *e*) from MCF-7 cells (cf. 6, 53, 55). The major of the two isoelectric variants of the transfected human CK 8 gene product comigrated with human CK 8 of MCF-7 cells; the other migrated as a somewhat more basic protein (Fig. 2, *d* and *e*).

To identify the truncated mutant CKs, we separated the [^{35}S]methionine-labeled in vitro translation products of RNAs synthesized in vitro from the corresponding CK cDNA constructs by two-dimensional gel electrophoresis. For example, Fig. 2 *b* shows the in vitro translation product of the tail-less human CK 8ΔT. The gel electrophoretic analysis of [^{35}S]methionine-labeled cytoskeletal proteins of 3T3-L1 cells doubly transfected with constructs coding for the tail-less CKs 8ΔT and 19 is shown in Fig. 2 *f*: here, the

Figure 3. Immunofluorescence microscopy showing the appearance of human CKs in murine 3T3-L1 cells stably transfected with gene constructs encoding CKs 8 and 18 (*a–d*) and CKs 8 and 19 (*e–g*), 65 h after plating. (*a*) Survey micrograph showing 3T3-L1 cells forming extended IF arrays containing CKs 8 and 18 as visualized by immunostaining with antibody lu-5. The inset in the lower right shows a mitotic cell in which part of the human CKs transiently appears in small granular aggregates (antibody K_s8.17.2). (*b*) Higher magnification showing details of organization of CK 8/18 fibrils in a transfected 3T3-L1 cell. (*c* and *d*) Double-label immunofluorescence of a transfected cell, reacted with monoclonal murine antibody lu-5 (followed by Texas Red–coupled goat anti-mouse IgG) for the detection of CKs (*c*) and guinea pig antibodies to vimentin (*d*; FITC-labeled). (*e–g*) IF meshworks formed by CKs 8 and 19, reacted with guinea pig antibodies against CK (*e*), monoclonal antibodies lu-5 (*f*), or K_s19.2-Z105 (*g*). Note the abundance of CK IFs (*e*) and the extensive IF meshworks formed (*f* and *g*). Bars: (*inset*, *a*; *f* and *g*) 10 μm; (*b*) 20 μm; (*a*) 25 μm; (*c*, *d*, and *e*) 50 μm.

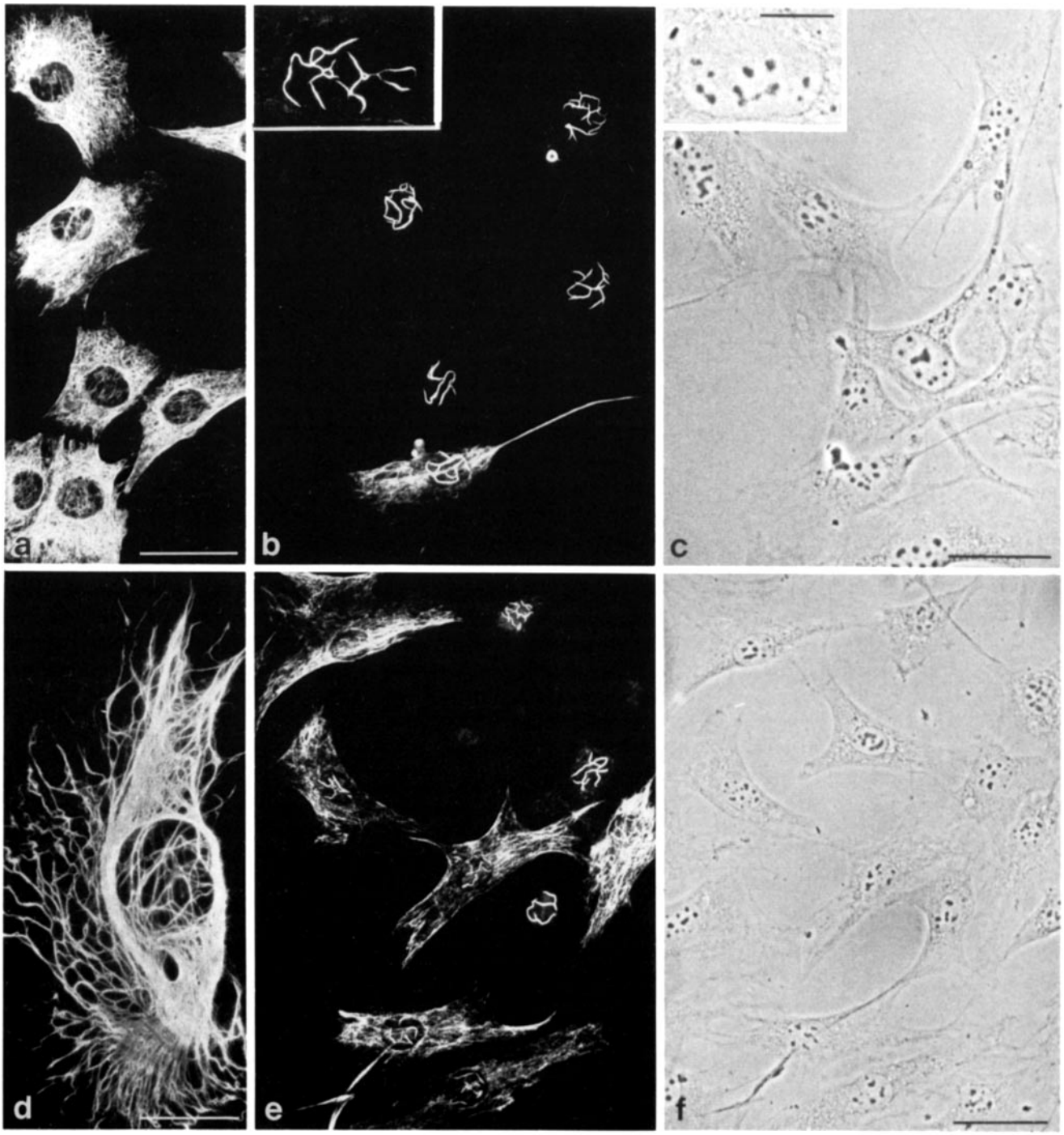

Figure 4. Arrays of CK IFs formed in murine 3T3-L1 cells stably transfected with cDNA constructs encoding tail-less human CKs such as CKs 8ΔT and 19, using different CK-specific antibodies (*a* and *d*, K_s19.2-Z105; *b* and *e*, lu-5). (*a*) Survey micrograph showing strong expression of the transfected genes in all cells of this field, with IFs extending over the cytoplasm but also appearing in or at the nucleus. (*b* and *c*) Epifluorescence (*b*) and phase contrast (*c*) micrographs of a subline in which most of the cells are positive for the foreign gene products (five out of eight cells; compare *b* with *c*) which appear here predominantly (four out of five cells) in the nuclei (as shown at higher magnification in the inset). (*d*) Higher magnification of a cell of the same subline as in *a*, showing the masses of CK fibrils which extend over the whole cytoplasm, although here a perinuclear accumulation is also obvious. (*e* and *f*) Epifluorescence (*e*) and phase contrast (*f*) micrographs, showing the coexistence of cells with an exclusively nuclear appearance of CK fibrils (3 out of 15), cells with CK fibrils occurring both in the nucleus and the cytoplasm (6 out of 15) and cells without any detectable CK structures. Bars: (*insets*, *b* and *c*; *d*) 25 μm; (*a–c*, *e*, and *f*) 50 μm.

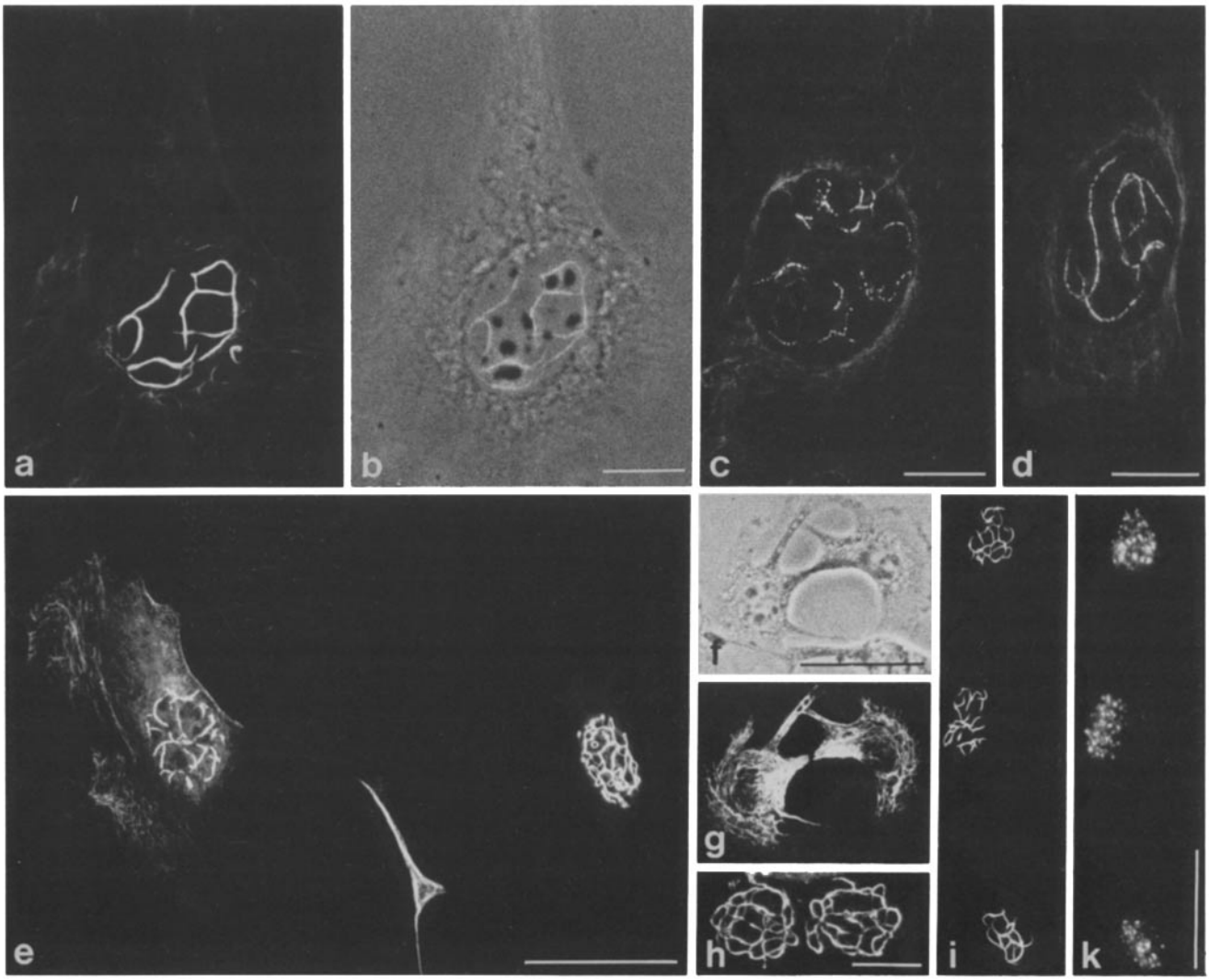

Figure 5. Details of the intranuclear appearance of IF structures formed de novo from stably transfected cDNA constructs encoding tail-less CKs, CK 8ΔT and CK 19, in normally grown and in colcemid-treated (*e* and *h*) cultures, as visualized with CK-specific monoclonal antibodies (*a–c* and *e–i*, lu-5; *d*, CAM 5.2). (*a* and *b*) Micrographs with epifluorescence (*a*) and combined epifluorescence-phase contrast (*b*) optics, showing the intranuclear location of the fibrillar CK-positive structures (*a*) in the same optical plane as the nucleoli and chromatin structures (*b*). (*c* and *d*) Various aspects of the intranuclear CK structures that appear as short (*c*) or long (*d*) linear arrays of granules ("beads-on-a-string"). (*e*) Intranuclear CK fibril arrays in colcemid-arrested cells, including reconstituted nuclei. (*f* and *g*) Two postmitotic daughter cells, seen in epifluorescence (*g*) and phase contrast (*f*), showing abundance of CK fibrils in the cytoplasm and virtual absence in the newly formed nuclei. (*h*) Binucleate cell after colcemid arrest, showing extensive CK fibrils in both nuclei. (*i* and *k*) Double-label fluorescence showing intranuclear CK fibrils visualized by CK antibodies (*i*) and chromatin structures visualized by staining with the DNA Hoechst dye (*k*). Note that the structures positive in *i* do not correspond to, or are associated with, those of (*k*). Bars: (*b–d* and *h*) 15 μm; (*e*, *f*, and *k*) 50 μm.

polypeptides of the tail-less CKs 8ΔT and 19 are identified in addition to vimentin.

Immunofluorescence Microscopy of Murine 3T3-L1 Cells Synthesizing Pairs of Intact Human CKs 8/18 or 8/19

By immunofluorescence microscopy with several monoclonal and CK-specific antibodies, including antibody lu-5 as well as several CK-specific antisera, we never have detected any fibrillar staining in untransfected 3T3-L1 cells or in cells single-transfected with a gene construct encoding either the type II CK 8 or the type I CKs 18 or 19 (data not shown; see also references 40, 41), in contrast to various other nonepithelial human cell lines in which CK 8 and/or 18 may appear in a variable proportion of cells.

Stably transfected 3T3-L1 cells synthesizing human CKs 8 and 18 (Fig. 3, *a–d*) or human CKs 8 and 19 (Fig. 3, *e–g*) showed an extensive fibrillar meshwork throughout the cytoplasm, not dissimilar from typical CK fibril arrays present in several epithelial cell lines (14, 16). During mitosis such filament arrays of transgenic CKs often changed in morphology and partly appeared in small granules, similar to those seen in diverse kinds of mitotic epithelial cells (Fig. 3 *a*, *inset*; 15, 46). During the time course of CK IF formation upon transfection we have not noticed conspicuous juxtanuclear aggregate(s) or central "IF organizing center(s)"

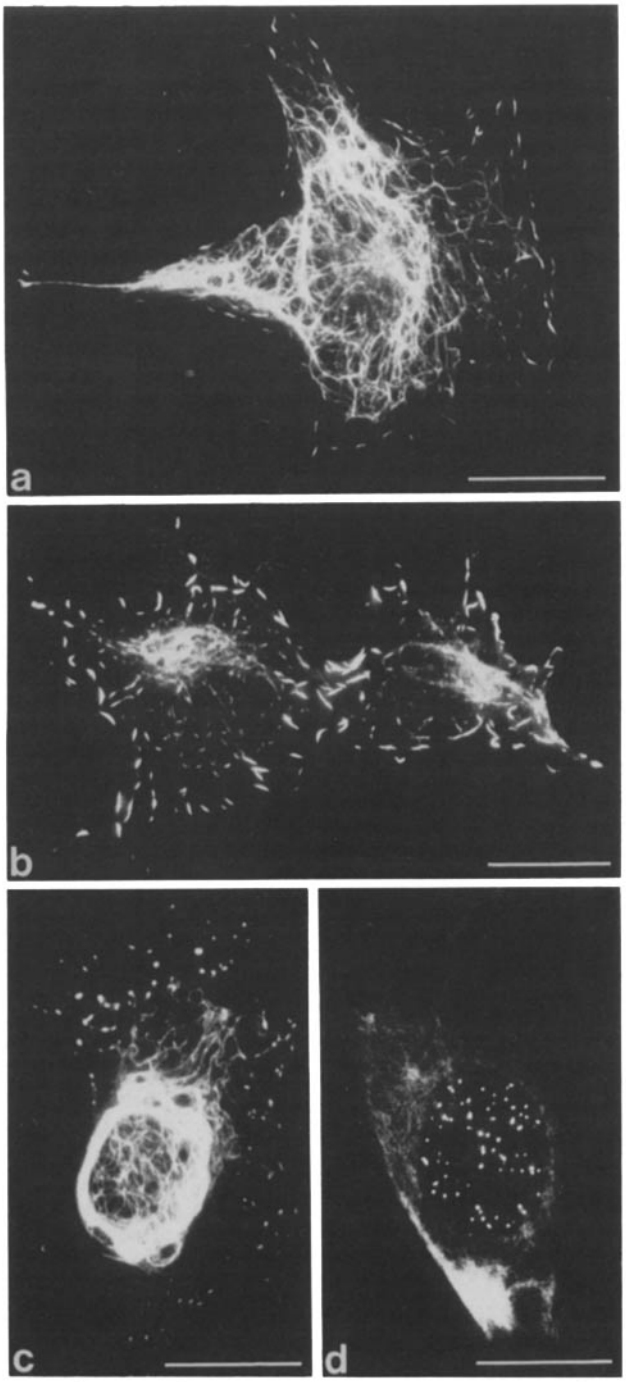

Figure 6. Immunofluorescence micrographs showing various forms of appearance of IF structures formed by tail-less human CKs 8ΔT and 18ΔT in transiently transfected cells immunostained with antibody lu-5, 65 h after transfection. (*a*) Extensive meshwork of CK IF bundles spread throughout the cell. (*b*) Daughter cells, displaying mostly short CK fibrils ("rods" and 'whiskers") in the cytoplasm, which are enriched at the cell periphery and in the perinuclear region. (*c*) Arrangement of extended and aggregated CK fibrils surrounding the nucleus, together with smaller CK structures ("dots") spread over the cytoplasm. (*d*) Accumulation of CK structures in both the cytoplasm and the nucleoplasm of the same cell. Here the cytoplasmic CK structures are concentrated in a large cytoplasmic aggregate (*bottom*), whereas the nuclear CKs appear in numerous small aggregates ("dots"). Bars, 25 μm.

(cf. 2, 3, 12) but rather disperse cytoplasmic rods, whiskers, and fibrils intensely stained with CK antibodies.

Double-label immunostaining with both CK- and vimentin-specific antibodies showed regions with locally different immunostaining but also far-reaching co-staining in other places (Fig. 3, *c* and *d*), suggesting, but not proving, the existence of both kinds of IF proteins in the same IF bundle array. Immunoelectron microscopy (see below), however, showed that the CK and vimentin IFs could be distinguished even when they occurred in closely parallel arrays, similar to our demonstrations of parallel arrays of CK IFs with desmin and vimentin IFs in other cell types (for example see reference 6).

Desmosomal plaque proteins were not detected in normal nor in transfected cells (data not shown).

These observations also indicate that the naturally tail-less CK 19 (5, 6) is a competent type I CK partner for CK 8, as these two polypeptides together form extended IF arrays, and that 3T3-L1 cells allow the synthesis of CKs and the formation of CK IFs.

Immunofluorescence Microscopy of Transfected 3T3-L1 Cells Synthesizing Domain-deleted Human CKs

When genes encoding the genetically engineered tail-less CK 8ΔT and the naturally tail-less CK 19 were co-expressed in 3T3-L1 cells, the resulting proteins formed massive arrays of IF bundles organized into extended cytoplasmic IF meshworks (Fig. 4, *a* and *d*). Again, when the time course of CK filament formation was examined, the earliest detectable CKs appeared as short whiskers throughout the cytoplasm, without any indication of a vectorial assembly from a nuclear envelope-associated IF-organizing center (data not shown).

Surprisingly, we consistently found that some of the cells synthesizing the tail-less CKs 8ΔT and 19 displayed spectacular fibrillar CK structures in the cell nucleus, either together with cytoplasmic CK IFs or exclusively nucleus confined (Fig. 4, *b*, *c*, *e*, and *f*). Nuclear CK immunostaining mostly appeared as relatively thick and intense reaction of individual fibrils (e.g., Fig. 4, *b* and *c*, *inset*, and Fig. 5, *a* and *b*), some of which could be traced for 10–20 μm. Less frequently, it was resolved into linear arrays of granular-looking CK deposits ("beads-on-a-string" arrays; Fig. 5, *c* and *d*).

Remarkably, most cell cultures were heterogeneous in this respect. Cells with nuclear CK fibrils occurred side-by-side with cells in which CK immunostaining occurred mostly or exclusively in the cytoplasm, and cells in which both nuclear and cytoplasmic CK fibrils co-existed were also seen (e.g., Fig. 4, *b*, *c*, *e*, and *f*). The relative distribution of these transgene CK IFs in the nucleus and/or the cytoplasm was obviously not restricted to telophase or G1 cells as nuclear IFs were also noticed in cells arrested with colcemid (Fig. 5, *e* and *h*) and in S-phase cells, as shown by colocalization with replication markers (not shown). Reversely, normal cytoplasmic IF arrays were also seen in the cytoplasm of postmitotic daughter cells (Fig. 5, *f* and *g*).

At the light microscopic level, the intranuclear CK IFs did not appear to be regularly associated with other nuclear structures such as nucleoli (for example, Figs. 4, *b* and *c*, and 5, *a* and *b*), chromatin (Fig. 5, *i* and *k*, shows direct com-

parison by double label with the DNA stain "Hoechst"), and the nuclear lamina, as demonstrable by double-labeling with lamin antibodies (data not shown).

The frequency of transfected cells with nuclear CK fibrils was variable for reasons not yet understood. For example, in stably transfectant clonal cultures at 25–35 passages after transfection and 2–3 clonal selections at minimal cell dilution and 4 d after cell plating, 40–55% of the cells showed positive CK fluorescence (this value was usually ~80% early after the first subcloning). Of those cells appearing CK positive, ~30% showed exclusively nuclear CK fibrils, ~20% showed exclusively cytoplasmic fibril reaction, and half of the cells appeared positive in the cytoplasm as well as in the nucleus.

When the synthesis of a tail-deleted CK 8ΔT together with tail-deleted CK 18ΔT was enforced in 3T3-L1 cells, either in transient (Fig. 6) or stable and selected (not shown) transfectants, a corresponding heterogeneous result was obtained: extensive cytoplasmic CK immunostaining (Fig. 6 *a*), the predominance of relatively short rod or whisker structures, often at the cell periphery (Fig. 6 *b*), co-existence of cytoplasmic fibrillar aggregates with cytoplasmic dots and whiskers (Fig. 6 *c*), or the appearance of nuclear CK structures, either in short fibrillar or in punctate arrays (for example Fig. 6 *d*).

When different other deletion CK cDNA constructs were similarly used for transfection of 3T3-L1 cells, the specific gene products appeared in the cytoplasm in all the head-deletions examined, either in a more disperse, apparently nonfibrillar pattern (Fig. 7 *a*, CK ΔH8 plus CK 19; Fig. 7, *g* and *h*, CK ΔH8 plus CK ΔH19 or CK ΔH18), in extended fibrils (Fig. 7 *b*, CK ΔH8 plus CK 18) in variously sized cytoplasmic granules (Fig. 7 *c*, CK ΔH8 plus CK 18; Fig. 7, *d–f*, CK 8 plus CK ΔH18), or in combinations of both (Fig. 7, *c* and *d*). In contrast, we observed CK gene products exclusively or predominantly in the nucleus in all those examples in which neither of the type I and type II CKs possessed a tail domain (Fig. 7, *i–r*). In these studies we noticed a great variety of forms of appearance of intranuclear CKs, from extended fibril-like masses (Fig. 7 *i*, CK 8ΔT plus CK ΔH19) to globular aggregates (Fig. 7 *l*, CK 8ΔT plus CK ΔH18ΔT) and finely punctate arrays (e.g., Fig. 7, *m–r*, CK ΔH8ΔT plus head- and tail-less type I CKs).

Electron Microscopy of Structures Formed by Transgenic and Tail-less Cytokeratins in Transfected Cells

The CK-containing structures formed in the transfected murine 3T3-L1 cells were routinely examined by electron microscopy of ultrathin sections, including pre-embedding immunolabeling with secondary antibodies coupled to ~5-nm colloidal gold particles. As expected from immunofluorescence microscopy, CK antibody label was found specifically on a certain subtype of cytoplasmic IF bundles (Fig. 8 *a*; *brackets* point to an example of a relatively thin bundle) or on densely packed bundles of IFs located deep in the nuclear interior (Fig. 8, *b* and *c*, *arrows*). Parallel experiments with vimentin antibodies showed gold labeling over a different kind of cytoplasmic IF bundles and were totally negative for the nucleus (not shown).

Because of the unusual appearance of CK fibrils in the nucleus we have documented these structures and their display with several heavy metal staining techniques. Typically, the intranuclear CKs appeared in often somewhat "wavy" and loosely packed IF bundles of various lengths (Fig. 9 *a* shows a near-longitudinal section of a long bundle). The individual IFs (7–12 nm) within these bundles were resolved in sufficiently thin sections (Fig. 9, *b–d*), and, for the most part, were practically indistinguishable from typical IFs nearby in the cytoplasm, with respect to diameter, surface appearance, and staining intensity (Fig. 9 *b*), except for some individual IFs which locally displayed regularly spaced particles on their surfaces (Fig. 9 *d*, *inset*). In a number of nuclei, the IF bundles were very abundant, running haphazardly through the nucleoplasm (Fig. 9 *e*). Close associations of IF bundles with chromatin structures were occasionally noticed at higher magnifications, but their significance was not clear.

Discussion

When, after gene transfection or mRNA microinjection, molecules of a type I CK meet type II CKs in a nonepithelial cell that does not express its own CK genes, they form heterotypic complexes and assemble into IFs arranged in bundles and meshworks. This shows that the formation of CK IF meshworks similar to those characteristic of epithelial cells does not require additional, epithelium-specific factors in agreement with previous injection and transfection experiments (28, 43, 45; see, however, reference 11) and with observations that CKs 8, 18, and 19 can be synthesized, spontaneously or after induction by some drugs or environmental factors, in certain nonepithelial cells during development and pathogenesis (6, 21, 40, 41). The CK tail deletion studies described here are also in agreement with the general concept of a requirement of an intact rod domain for IF formation (2, 3, 8, 51, 73).

From our results we conclude that CK polypeptides lacking the tail domain in both partners of the heterotypic complex can form sufficiently high CK concentration provided normal-looking IFs which laterally associate into conspicuous bundles and form extensive fibrillar meshworks. This conclusion is based on observations of the de novo formation of IFs in cells of a nonepithelial line, mouse 3T3-L1, upon transfections with gene constructs that encode human CKs lacking the tail domain either naturally (CK 19) or as the result of genetic manipulations (CK 8ΔT and CK 18ΔT). In these experiments, the heterotypic combination of tail-deleted CK 8 (CK 8ΔT) with tail-deleted CK 18 (CK 18ΔT) has been successful in both protein stabilization (for discussion of heterotypic requirements, see references 11, 40, 41, 44, 45, 48, 51) and IF formation as is true with the naturally tail-less CK 19. (For the very short extension at the end of the rod, ranging from 1 amino acid in *Xenopus laevis* to 13 in the mammalian protein, see references 5, 6, 13, 68.) As we have controlled the resulting truncated proteins by gel electrophoresis and immunoblotting and as we have not noticed any murine CK to appear in the transfected cells, we are convinced that the cytoskeletal IFs visualized by CK antibodies contain the tail-less CKs.

Our results are in agreement with the recent in vitro filament reconstitution experiments of Hatzfeld and Weber (33) who have reported that purified, tail-truncated CK 8 can assemble, when combined with purified CK 19, into normal-

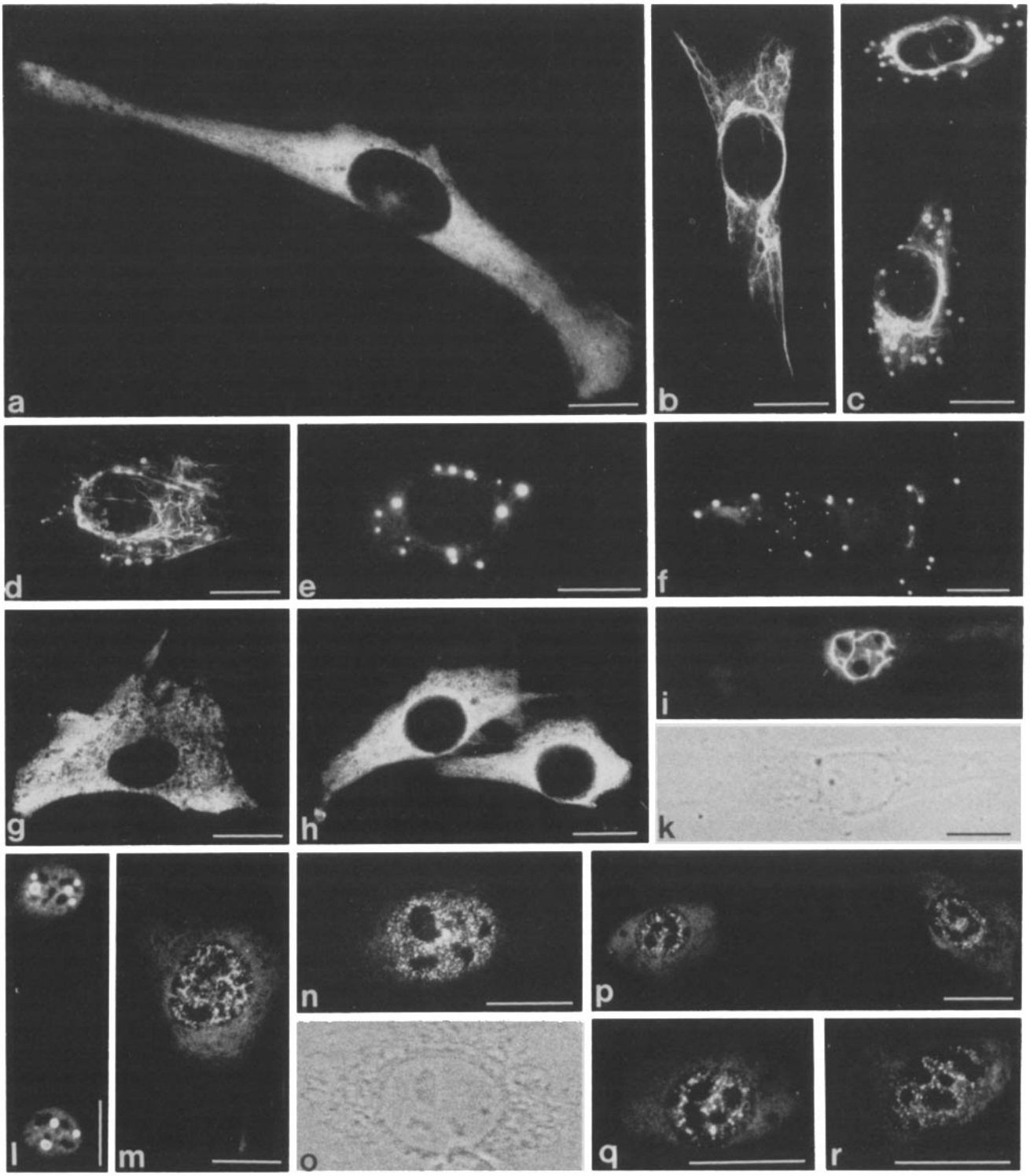

Figure 7. Intracellular distribution of CK structures formed from variously deleted CKs encoded by human CK gene constructs, after transfection of mouse 3T3-L1 cells, as visualized by immunofluorescence microscopy using CK antibody lu-5. (*a*) Headless CK 8 and naturally tail-less CK 19, showing exclusively cytoplasmic CKs which here are not integrated into a fibrillar meshwork. (*b* and *c*) Headless CK 8 with normal CK 18, showing exclusively cytoplasmic fibrils (*b*) or cytoplasmic fibrils together with granular structures (*c*). (*d–f*) Intact CK 8 with headless CK 18, showing exclusively cytoplasmic gene products, with various proportions of fibrillar and granular structures, from predominantly fibrillar (*d*) to juxtanuclear granules (*e*) and dispersed granules (*f*). (*g* and *h*) Headless CK 8 with headless CK 19 (*g*) or headless CK 18 (*h*), showing CKs restricted to the cytoplasm, but in a more diffuse appearance and not in the form of a fibrillar meshwork. (*i* and *k*) Tail-less CK 8 with a headless mutation of the naturally tail-less CK 19, showing nuclear enrichment (*i*, fluorescence; *k*, phase contrast). (*l*) Tail-less CK 8 combined with a head- and tail-less CK 18 mutant, showing nuclear enrichment of CKs, most of which is concentrated in spheroidal aggregates. (*m*) Structures formed from head- and tail-less CK 8 together with CK 19, showing most of the CK immunofluorescence in the nucleus where it appears in bizarre arrays of punctate substructures. (*n* and *o*) Head- and tail-less CK 8, as in *m*, but combined with headless CK 19, showing immunostaining of nuclear CKs in punctate arrays extending through the

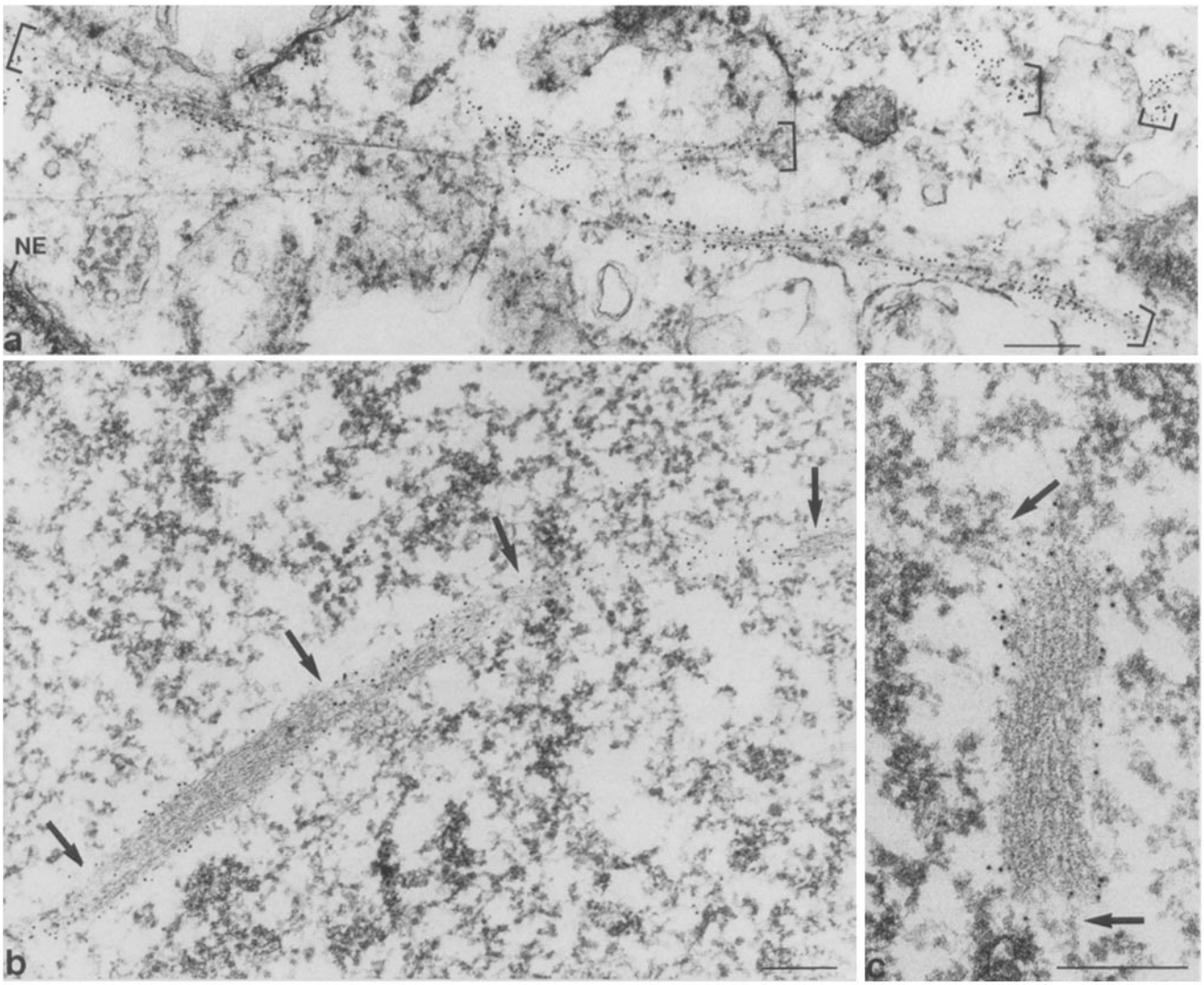

Figure 8. Immunoelectron microscopy (pre-embedding reactions) of ultrathin sections, showing CK fibrils formed from tail-less human CKs 8ΔT and 19 in the cytoplasm (*a*) and the nucleoplasm (*b* and *c*) of stably transfected murine 3T3-L1 cells. *NE*, nuclear envelope. (*a*) Cytoplasmic CK IF bundles (*brackets*) identified by immunoreaction with antibody lu-5, followed by decoration with 5-nm colloidal gold–conjugated goat anti-mouse IgG. Adjacent, often parallel vimentin IFs are not decorated by gold particles. (*b*) Typical fibril bundles of densely packed CK IFs (*arrows*) in the nucleoplasm. (*c*) Higher magnification of such a dense CK IF bundle in close proximity to chromatin structures (*arrows*). Bars, 0.2 μm.

looking IFs. However, they appear to be at variance with the conclusion of Lu and Lane (51) from gene infection experiments, using deletion mutants similar, but not identical to ours in a retroviral vector that "within a keratin pair one of the proteins must have both end domains" to produce extended IF meshworks. In their experiments, these authors have, however, also noticed that only "short kinked filamentous structures" are seen in NIH 3T3 cells infected with gene constructs encoding natural CK 19 and a mutant CK 8 from which the last two thirds of the tail domain had been deleted. Whether these short kinked fibrillar structures represent correct IFs, although not assembled into a higher order meshwork of fibrils, has not been examined by these authors (51) by electron microscopy (for a demonstration that even light microscopically "globular" structures can be composed of IFs; see reference 53).

At present, we have no satisfactory explanation for these different results. They may be due to different levels of expression of one or both of the heterotypic CK partners, as we have repeatedly observed short CK IF whiskers in individual cells that were not (yet) integrated into a typical meshwork, and this was more frequently seen at early times after transfection. Similarly, numerous short IF structures spread over the cytoplasm have been noticed at early time

nucleoplasm, leaving the nucleoli unstained (*n*, epifluorescence; *o*, phase contrast). (*p–r*) The combination of "only rods" mutations, i.e., head- and tail-less CKs 8 and 18, also results in a marked nuclear enrichment of structures formed from the defect CKs (*p*) which, at higher magnification (*q* presents a partial blow up of the left nucleus of *p*; *r* shows a different cell) are resolved into complex arrays of CK-positive granules similar to those seen in *m* and *n*. Bars, 20 μm.

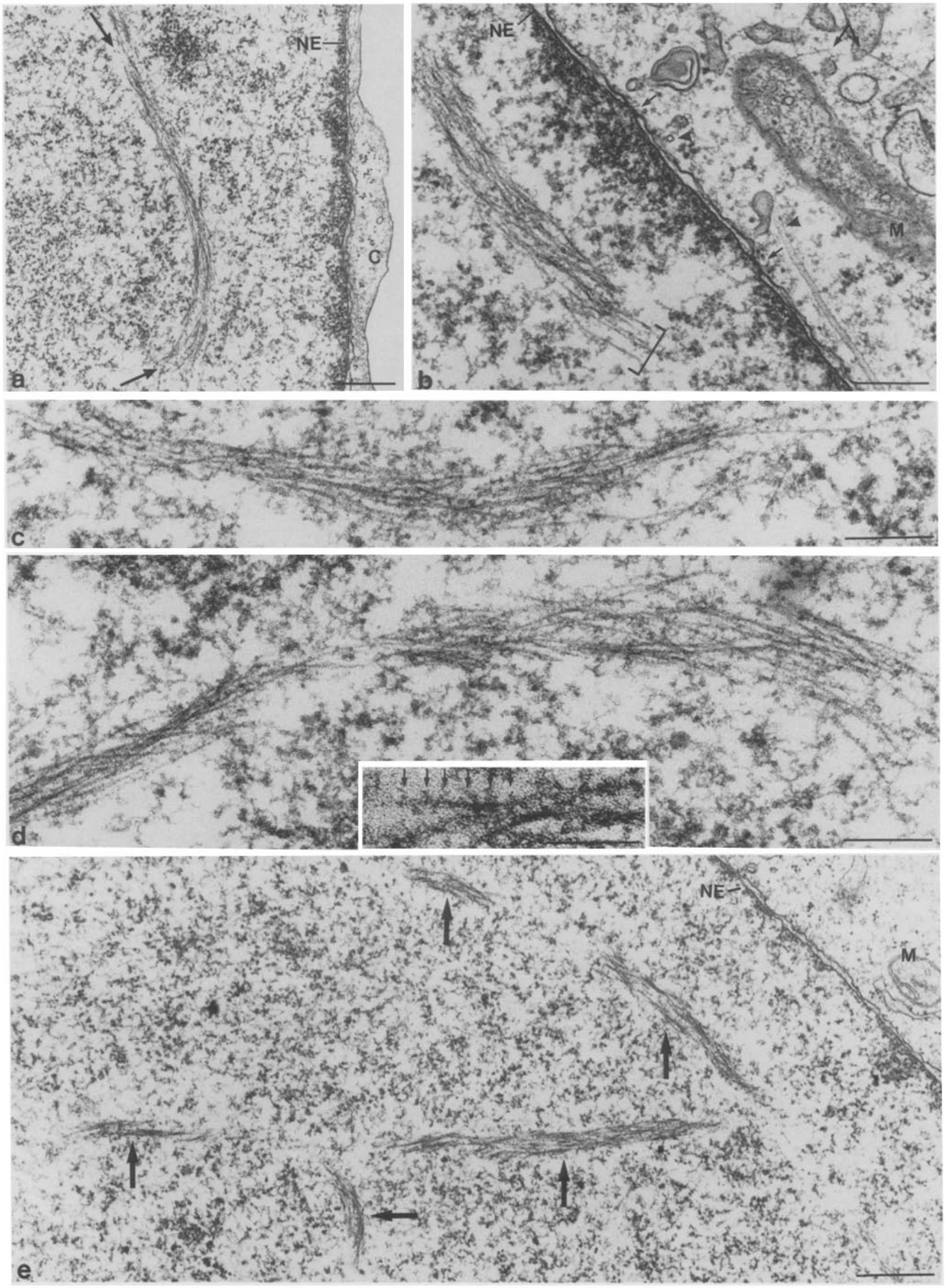
NE
C
a
NE
A
M
b
c
d
NE
M
e

points after microinjection of CK mRNA injection (43) and in the desmin gene transfection experiments of Raats et al. (in reference 62, see Fig. 7). Clearly, this appearance of short IF structures formed de novo at multiple sites throughout the cytoplasm speaks against the requirement of a dominant juxtanuclear "IF organizing center" proposed by others (2, 12; see, however, also reference 58).

Our conclusion that the tail domain of the CKs examined, e.g., CKs 8, 18, and 19, is not required for the formation of IFs and IF bundles, cannot be generalized a priori to other IF proteins and to other kinds of cells. In extensive transfection experiments, using gene constructs with a *myc* motif as a "tag," Cleveland and colleagues (27, 77) have reported that molecules of neurofilament protein NF-L lacking about half of the tail domain could disturb the structural appearance of an IF meshwork of the vimentin:NF-L heteropolymers in ~70% of the cells. In contrast, 80% of the cells showed normal IF meshworks when vimentin was allowed to mix with a transgenic neurofilament protein NF-M version from which almost the entire tail (down to a residual stump of nine amino acids) had been removed.

The observation that in 3T3-L1 cells forced to produce CKs without a tail domain, extensive bundles of CK filaments indistinguishable from cytoplasmic IFs often appear in the nucleus where they can be organized in extensive IF bundle arrays has been a surprise. In many cells, the nucleus was the only compartment in which CK IFs were detected, although these cells showed a normal cytoplasmic meshwork of vimentin IFs. In other cells, extensive CK IF bundles were seen in both compartments, the nucleoplasm and the cytoplasm. These observations and the finding that a third category of cells from the same clone displayed the normal cytoplasmic restriction of CK IFs, indicate that nuclear IF accumulation is not an obligatory consequence of the tail truncation. Rather, our observations suggest to us that tail-deletion results, permissively, in a relaxation of the normal cytoplasmic restriction in many of the transfected cells, probably due to a release from restrictive interactions. The similarity of this nuclear IF appearance with the formation of intranuclear microfilament bundles upon treatment of cells with DMSO is apparent (cf. 24, 59, 64).

These intranuclear IFs are not associated with the nuclear lamina, and in double-label experiments using antibodies to CKs and lamins we have not noticed any lamin co-localization with the intranuclear CK bundles (data not shown). Therefore, we do not assume that the appearance of such masses of CK IFs within the nucleoplasm involves the formation, if only transient, of CK:lamin copolymers. We have also not noticed a specific association of these nuclear CK IFs with any nuclear substructures, although occasional contacts with chromatin are suggested in some places (for in vitro binding of IF proteins to single-stranded nucleic acids see reference 57). Obviously, there is not an apparent interference of the intranuclear CK IFs with the proliferation and any of the important nuclear functions of the transfected 3T3-L1 cells.

We want to emphasize, however, that this appearance of IF bundles throughout the nucleoplasm is a specific result that, in such transfection experiments, is obviously related to the absence of tail domains in otherwise complete CKs. Moreover, the situation of the nuclear IFs shown here is fundamentally different from reports of diffuse CK 8-like immunoreactivity in the nuclear matrix (4), the CK 19 association with chromatin and/or nuclear lamina (75). Punctate arrays of nuclear antigens reactive with a specific desmin antibody have been described by Kamei (38). However, in none of these studies has an IF nature of the nuclear structures under question been demonstrated. While CKs that lacked not only tails but also head domains were also seen in the nuclear interior, they mostly appeared in different forms, predominantly globular or finely punctate; we are currently determining, by immunoelectron microscopy, these peculiar CK deposits but have so far not detected any typical IF structures. In our experiments, we have also never observed head-deleted CKs with intact tails in the nucleus. On the other hand, Albers and Fuchs (3) have reported, after transfection of a tag-coupled, head-truncated human CK14, dot-like CK structures at the nuclear surface or in the nuclear interior, but these authors did not determine the exact location and the ultrastructural form of these dots.

The appearance of an insoluble (cytoskeletal) protein polymer structure within the confinements of the nuclear envelope raises the question of the mechanism of its formation. Clearly, the CK molecules do not contain a nuclear accumulation signal characteristic of diverse kinds of nuclear proteins (for recent review see reference 66). If one assumes that these intranuclear IFs are formed by local assembly of diffusible states of CK molecules that have distributed between nucleus and cytoplasm, one has to face the canonical dogma of an upper size exclusion limit for nuclear uptake of a molecular weight of ~60,000 which is clearly below the molecular size of coiled-coil CK dimers or tetramers; i.e., the most probable states of existence of soluble IF proteins in the cytoplasm (e.g. 8, 19, 25, 67). It remains to be examined whether the tail-truncated CKs described here indeed exist, and enter the nucleus, as oligomeric coiled-coil associations, or whether they pass the nuclear pore complexes as "piggy-back" complexes with certain nucleus-specific proteins.

Our observation of the appearance of IFs in the nucleo-

Figure 9. Electron micrographs of sections of normally fixed and processed cells, showing various aspects of CK IF bundles formed in nuclei of murine 3T3-L1 cells synthesizing tail-less human CKs 8ΔT and 19. (*a*) Survey micrograph showing a typical long CK IF bundle (*arrows*) in the nucleoplasm. *C*, cytoplasm; *NE*, nuclear envelope. (*b*) Higher magnification picture, showing details of a nuclear CK filament bundle (*bracket*) in the vicinity of the nuclear envelope (*small arrows* point to nuclear pore complexes). Note that the nuclear IFs are of the same diameter as the cytoplasmic IFs (two are denoted by the bifurcation symbol in the upper right). Other symbols are as in *a*. *M*, mitochondrion. *Arrowheads*, microtubules in cross- and longitudinal sections. (*c* and *d*) Higher magnification of loosely arranged nuclear CK IF bundles, allowing the tracing of individual filaments for considerable distances. Note the typical "wavy" appearance of the bundles, their occasional close associations with nucleoplasmic particle structures and locally restricted regular arrays of projections (*d*; and inset *d*, arrows). (*e*) Survey micrograph showing the frequence of CK IF bundles (*arrows*) that traverse the nucleoplasm in different directions. Symbols as in previous figures. Bars: (inset in *d*) 0.1 μm; (*b–d*) 0.2 μm; (*a* and *e*) 0.5 μm.

plasm when CKs lacking tail domains are introduced into a cell normally devoid of CKs, also points to a possible structural function, albeit auxiliary, of the tail domain. As it is widely assumed that the tail domains of IF proteins protrude from the filament backbone and interact with other cell components, the appearance of soluble tail-less CKs in the nucleus and their assembly into CK IFs might result from the lack of association with, and retention on, cytoplasmic "anchorage" structures. Direct binding experiments are underway to test this possibility.

We thank Jutta Müller-Osterholt for excellent photographic work; and Dr. Harald Herrmann and Mrs. Ilse Hofmann for valuable discussions. We also gratefully acknowledge the careful typing of the manuscript by Eva Gundel.

The work has been supported in part by a grant from the Deutsche Forschungsgemeinschaft (DFG).

Received for publication 26 April 1991 and in revised form 19 August 1991.

References

1. Aebi, U., M. Häner, J. Troncoso, R. Eichner, and A. Engel. 1988. Unifying principles in intermediate filament (IF) structure and assembly. *Protoplasma (Berl.).* 145:73–81.
2. Albers, K., and E. Fuchs. 1987. The expression of mutant epidermal keratin cDNAs transfected in simple epithelial and squamous cell carcinoma lines. *J. Cell Biol.* 105:791–806.
3. Albers, K., and E. Fuchs. 1989. Expression of mutant keratin cDNAs in epithelial cells reveals possible mechanisms for initiation and assembly of intermediate filaments. *J. Cell Biol.* 108:1477–1493.
4. Aligué, R., R. Bastos, J. Serratosa, C. Enrich, P. James, C. Pujades, and O. Bachs. 1990. Increase in a 55-kDa keratin-like protein in the nuclear matrix of rat liver cells during proliferative activation. *Exp. Cell Res.* 186:346–353.
5. Bader, B. L., T. M. Magin, M. Hatzfeld, and W. W. Franke. 1986. Amino acid sequence and gene organization of cytokeratin no. 19, an exceptional tail-less intermediate filament protein. *EMBO (Eur. Mol. Biol. Organ.) J.* 5:1865–1875.
6. Bader, B. L., L. Jahn, and W. W. Franke. 1988. Low level expression of cytokeratins 8, 18 and 19 in vascular smooth muscle cells of human umbilical cord and in cultured cells derived therefrom, with an analysis of the chromosomal locus containing the cytokeratin 19 gene. *Eur. J. Cell Biol.* 47:300–319.
7. Birkenberger, L., and W. Ip. 1990. Properties of the desmin tail domain: studies using synthetic peptides and antipeptide antibodies. *J. Cell Biol.* 111:2063–2075.
8. Coulombe, P. A., Y.-M. Chan, K. Albers, and E. Fuchs. 1990. Deletions in epidermal keratins leading to alterations in filament organization in vivo and in intermediate filament assembly in vitro. *J. Cell Biol.* 111: 3049–3064.
9. Cowin, P., H.-P. Kapprell, W. W. Franke, J. Tamkun, and R. O. Hynes. 1986. Plakoglobin, a protein common to different kinds of intercellular adhering junctions. *Cell.* 46:1063–1073.
10. Crewther, W. G., L. M. Dowling, P. M. Steinert, and D. A. D. Parry. 1983. Structure of intermediate filaments. *Int. J. Biol. Macromol.* 5: 267–274.
11. Domenjoud, L., J. L. Jorcano, B. Breuer, and A. Alonso. 1988. Synthesis and fate of keratins 8 and 18 in nonepithelial cells transfected with cDNA. *Exp. Cell Res.* 179:352–361.
12. Eckert, B. S., R. A. Daley, and L. M. Parysek. 1982. Assembly of keratin onto PtK_1 cytoskeletons: evidence for an intermediate filament organizing center. *J. Cell Biol.* 92:575–578.
13. Eckert, R. L. 1988. Sequence of the human 40-kDa keratin reveals an unusual structure with very high sequence identity to the corresponding bovine keratin. *Proc. Natl. Acad. Sci. USA.* 85:1114–1118.
14. Franke, W. W., K. Weber, M. Osborn, E. Schmid, and C. Freudenstein. 1978. Antibody to prekeratin. Decoration of tonofilament-like arrays in various cells of epithelial character. *Exp. Cell Res.* 116:429–445.
15. Franke, W. W., E. Schmid, C. Grund, and B. Geiger. 1982*a*. Intermediate filament proteins in nonfilamentous structures: transient disintegration and inclusion of subunit proteins in granular aggregates. *Cell.* 30:103–113.
16. Franke, W. W., E. Schmid, D. L. Schiller, S. Winter, E.-D. Jarasch, R. Moll, H. Denk, B. W. Jackson, and K. Illmensee. 1982*b*. Differentiation-related patterns of expression of proteins of intermediate-size filaments in tissues and cultured cells. *Cold Spring Harbor Symp. Quant. Biol.* 46:431–453.
17. Franke, W. W., E. Schmid, S. Mittnacht, C. Grund, and J. L. Jorcano. 1984. Integration of different keratins into the same filament system after microinjection of mRNA for epidermal keratins into kidney epithelial cells. *Cell.* 36:813–825.
18. Franke, W. W., M. Hergt, and C. Grund. 1987*a*. Rearrangement of the vimentin cytoskeleton during adipose conversion: formation of an intermediate filament cage around lipid globules. *Cell.* 49:131–141.
19. Franke, W. W., S. Winter, E. Schmid, P. Soellner, G. Haemmerling, and T. Achtstaetter. 1987*b*. Monoclonal cytokeratin antibody recognizing a heterotypic complex: immunological probing of conformational states of cytoskeletal proteins in filaments and in solution. *Exp. Cell Res.* 173: 17–37.
20. Franke, W. W., S. Winter, J. van Overbeck, F. Gudat, P. U. Heitz, and C. Stähli. 1987*c*. Identification of the conserved, conformation-dependent cytokeratin epitope recognized by monoclonal antibody (lu-5). *Virchows Arch. A.* 411:137–147.
21. Franke, W. W., L. Jahn, and A. C. Knapp. 1989. Cytokeratins and desmosomal proteins in certain epithelioid and nonepithelial cells. *In* Cytoskeletal Proteins in Tumor Diagnosis. M. Osborn and K. Weber, editors. Cold Spring Harbor Laboratory Press, Cold Spring Harbor, NY. 151–172.
22. Frohmann, M. A., M. K. Dush, and G. R. Martin. 1988. Rapid production of full-length cDNAs from rare transcripts. Amplification using a single gene-specific oligonucleotide primer. *Proc. Natl. Acad. Sci. USA.* 85: 8998–9002.
23. Fuchs, E., A. L. Tyner, G. J. Giudice, D. Marchuk, A. RayChaudhury, and M. Rosenberg. 1987. The human keratin genes and their differential expression. *Curr. Top. Dev. Biol.* 22:5–34.
24. Fukui, Y., and H. Katsumaru. 1979. Nuclear actin bundles in *Amoeba*, *Dictyostelium* and human HeLa cells induced by dimethyl sulfoxide. *Exp. Cell Res.* 120:451–455.
25. Gall, L., and E. Karsenti. 1987. Soluble cytokeratins in *Xenopus laevis* oocytes and eggs. *Biol. Cell.* 61:33–38.
26. Geisler, N., E. Kaufmann, and K. Weber. 1982. Proteinchemical characterization of three structurally distinct domains along the protofilament unit of desmin 10 nm filaments. *Cell.* 30:277–286.
27. Gill, S. R., P. C. Wong, M. J. Monteiro, and D. W. Cleveland. 1990. Assembly properties of dominant and recessive mutations in the small mouse neurofilament (NF-L) subunit. *J. Cell Biol.* 111:2005–2019.
28. Giudice, G. J., and E. Fuchs. 1987. The transfection of epidermal keratin genes into fibroblasts and simple epithelial cells: evidence for inducing a type I keratin by a type II gene. *Cell.* 48:453–463.
29. Gorman, C. 1985. High efficiency gene transfer into mammalian cells. *In* DNA Cloning, Vol. II: A Practical Approach. D. M. Glover, editor. IRL Press, New York. 143–165.
30. Green, H., and M. Meuth. 1974. An established pre-adipose cell line and its differentiation in culture. *Cell.* 3:127–133.
31. Gunning, P., J. Leavitt, G. Muscat, S.-Y. Ng, and L. Kedes. 1987. A human beta-actin expression vector system directs high-level accumulation of antisense transcripts. *Proc. Natl. Acad. Sci. USA.* 84:4831–4835.
32. Hatzfeld, M., and W. W. Franke. 1985. Pair formation and promiscuity of cytokeratins: formation in vitro of heterotypic complexes and intermediate-sized filaments by homologous and heterologous recombinations of purified polypeptides. *J. Cell Biol.* 101:1826–1841.
33. Hatzfeld, M., and K. Weber. 1990. Tailless keratins assemble into regular intermediate filaments *in vitro*. *J. Cell Sci.* 97:317–324.
34. Hatzfeld, M., G. Maier, and W. W. Franke. 1987. Cytokeratin domains involved in heterotypic complex formation determined by in vitro binding assays. *J. Mol. Biol.* 197:237–255.
35. Heid, H. W., I. Moll, and W. W. Franke. 1988. Patterns of expression of trichocytic and epithelial cytokeratins in mammalian tissues. I. Human and bovine hair follicles. *Differentiation.* 37:137–157.
36. Hisanaga, S.-I., and N. Hirokawa. 1988. Structure of the peripheral domains of neurofilaments revealed by low angle rotary shadowing. *J. Mol. Biol.* 202:297–305.
37. Hisanaga, S.-I., and N. Hirokawa. 1990. Molecular architecture of the neurofilament. II. Reassembly process of neurofilament L protein *in vitro*. *J. Mol. Biol.* 211:871–882.
38. Kamei, H. 1990. Location of nuclear antigen(s) recognized by DSB389 MAb, a monoclonal antibody against desmin, observed by confocal laser scanning fluorescence microscopy. *Cell Biol. Int. Rep.* 14:727–736.
39. Kaufmann, E., K. Weber, and N. Geisler. 1985. Intermediate filament forming ability of desmin derivatives lacking either the amino-terminal 67 or the carboxy-terminal 27 residues. *J. Mol. Biol.* 185:733–742.
40. Knapp, A. C., and W. W. Franke. 1989. Spontaneous losses of control of cytokeratin gene expression in transformed, non-epithelial human cells occurring at different levels of regulation. *Cell.* 59:67–79.
41. Knapp, A. C., F. X. Bosch, M. Hergt, C. Kuhn, S. Winter-Simanowski, E. Schmid, S. Regauer, J. Bartek, and W. W. Franke. 1989. Cytokeratins and cytokeratin filaments in subpopulations of cultured human and rodent cells of nonepithelial origin: modes and patterns of formation. *Differentiation.* 42:81–102.
42. Krauss, S., and W. W. Franke. 1990. Organization and sequence of the human gene encoding cytokeratin 8. *Gene.* 86:241–249.
43. Kreis, T. E., B. Geiger, E. Schmid, J. L. Jorcano, and W. W. Franke.

1983. De novo synthesis and specific assembly of keratin filaments in nonepithelial cells after microinjection of mRNA for epidermal keratin. *Cell.* 32:1125–1137.

44. Kulesh, D. A., and R. G. Oshima. 1988. Cloning of the human keratin 18 gene and its expression in nonepithelial mouse cells. *Mol. Cell. Biol.* 8:1540–1550.
45. Kulesh, D. A., G. Ceceña, Y. M. Darmon, M. Vasseur, and R. G. Oshima. 1989. Posttranslational regulation of keratins: degradation of mouse and human keratins 18 and 8. *Mol. Cell Biol.* 9:1553–1565.
46. Lane, E. B., S. L. Goodman, and L. K. Trejdosiewicz. 1982. Disruption of the keratin filament network during epithelial cell divisions. *EMBO (Eur. Mol. Biol. Organ.) J.* 1:1365–1372.
47. Lee, C. C., and C. T. Caskey. 1990. cDNA cloning using degenerate primers. *In* PCR Protocols. M. A. Innis, D. H. Gelfand, J. J. Sninsky, T. J. White, editors. Academic Press, Inc., San Diego, CA. 46–59.
48. Lersch, R., V. Stellmach, C. Stocks, G. Giudice, and E. Fuchs. 1989. Isolation, sequence, and expression of a human keratin K5 gene: transcriptional regulation of keratins and insights into pairwise control. *Mol. Cell Biol.* 9:3685–3697.
49. Leube, R. E., F. X. Bosch, V. Romano, R. Zimbelmann, H. Höfler, and W. W. Franke. 1986. Cytokeratin expression in simple epithelia. III. Detection of mRNAs encoding human cytokeratins nos. 8 and 18 in normal and tumor cells by hybridization with cDNA sequences in vitro and in situ. *Differentiation.* 33:69–85.
50. Leube, R. E., B. L. Bader, F. X. Bosch, R. Zimbelmann, T. Achtstätter, and W. W. Franke. 1988. Molecular characterization and expression of the stratification-related cytokeratins 4 and 15. *J. Cell Biol.* 106:1249–1261.
51. Lu, X., and B. Lane. 1990. Retrovirus-mediated transgenic keratin expression in cultured fibroblasts: specific domain functions in keratin stabilization and filament formation. *Cell.* 62:681–696.
52. Magin, T. M., M. Hatzfeld, and W. W. Franke. 1987. Analysis of cytokeratin domains by cloning and expression of intact and deleted polypeptides in *Escherichia coli*. *EMBO (Eur. Mol. Biol. Organ.) J.* 6:2607–2615.
53. Magin, T. M., B. L. Bader, M. Freudenmann, and W. W. Franke. 1990. De novo formation of cytokeratin filaments in calf lens cells and cytoplasts after transfection with cDNAs or microinjection with mRNAs encoding human cytokeratins. *Eur. J. Cell Biol.* 53:333–348.
54. McKeon, F. 1991. Nuclear lamin proteins: domains required for nuclear targeting, assembly, and cell-cycle-regulated dynamics. *Curr. Opin. Cell Biol.* 3:82–86.
55. Moll, R., W. W. Franke, D. L. Schiller, B. Geiger, and R. Krepler. 1982. The catalog of human cytokeratins: patterns of expression in normal epithelia, tumors and cultured cells. *Cell.* 31:11–24.
56. Moll, R., D. L. Schiller, and W. W. Franke. 1990. Identification of protein IT of the intestinal cytoskeleton as a novel type I cytokeratin with unusual properties and expression patterns. *J. Cell Biol.* 111:567–580.
57. Nelson, W. J., and P. Traub. 1982. Intermediate (10 nm) filament proteins and the Ca^{2+}-activated proteinase specific for vimentin and desmin in the cells from fish to man: an example of evolutionary conservation. *J. Cell Sci.* 57:25–49.
58. Ngai, J., T. R. Coleman, and E. Lazarides. 1990. Localization of newly synthesized vimentin subunits reveals a novel mechanism of intermediate filament assembly. *Cell.* 60:415–427.
59. Osborn, M., and K. Weber. 1980. Dimethylsulfoxide and the ionophore A23187 affect the arrangement of actin and induce nuclear actin paracrystals in PtK2 cells. *Exp. Cell Res.* 129:103–114.
60. Oshima, R. G., J. L. Millán, and G. Ceceña. 1986. Comparison of mouse and human keratin 18: a component of intermediate filaments expressed prior to implantation. *Differentiation.* 33:61–68.
61. Quinlan, R. A., R. D. Moir, and M. Stewart, 1989. Expression in *Escherichia coli* of fragments of glial fibrillary acidic protein: characterization, assembly properties and paracrystal formation. *J. Cell Sci.* 93:71–83.
62. Raats, J. M., F. R. Pieper, W. T. M. Vree-Egberts, K. N. Verrijp, F. C. S. Ramaekers, and H. Bloemendal. 1990. Assembly of amino-terminally deleted desmin in vimentin-free cells. *J. Cell Biol.* 111:1971–1985.
63. Saeed, T., and W. Ip. 1989. Assembly properties of two CNBr fragments of avian desmin that correspond to the headpiece domain and helix 1B. *Biochem. Biophys. Res. Commun.* 165:1059–1066.
64. Sanger, J. W., J. M. Sanger, T. E. Kreis, and B. M. Jockusch. 1980. Reversible translocation of cytoplasmic actin into the nucleus caused by dimethyl sulfoxide. *Proc. Natl. Acad. Sci. USA.* 77:5268–5272.
65. Shoeman, R. L., E. Mothes, C. Kesselmeier, and P. Traub. 1990. Intermediate filament assembly and stability *in vitro*: effect and implications of the removal of head and tail domains of vimentin by the human immunodeficiency virus type 1 protease. *Cell Biol. Int. Rep.* 14:583–594.
66. Silver, P. 1991. How proteins enter the nucleus. *Cell.* 64:489–497.
67. Soellner, P., R. A. Quinlan, and W. W. Franke. 1985. Identification of a distinct soluble subunit of an intermediate filament protein: tetrameric vimentin from living cells. *Proc. Natl. Acad. Sci. USA.* 82:7929–7933.
68. Stasiak, P. C., and E. B. Lane. 1987. Sequence of cDNA coding for human keratin 19. *Nucleic Acids Res.* 15:10058.
69. Steinert, P. M., and D. R. Roop. 1988. Molecular and cellular biology of intermediate filaments. *Annu. Rev. Biochem.* 57:593–625.
70. Steven, A. C., J. F. Hainfeld, B. L. Trus, J. S. Wall, and P. M. Steinert. 1985. Conformity and diversity in the structures of intermediate filaments. *Ann. NY Acad. Sci.* 455:371–380.
71. Stewart, M., R. A. Quinlan, and R. D. Moir. 1989. Molecular interactions in paracrystals of a fragment corresponding to the α-helical coiled-coil rod portion of glial fibrillary acidic protein: evidence for an antiparallel packing of molecules and polymorphism related to intermediate filament structure. *J. Cell Biol.* 109:225–243.
72. Traub, P., and C. E. Vorgias. 1983. Involvement of the N-terminal polypeptide of vimentin in the formation of intermediate filaments. *J. Cell Sci.* 63:43–67.
73. Trevor, K. T. 1990. Disruption of keratin filaments in embryonic epithelial cell types. *New Biol.* 2:1004–1014.
74. Van den Heuvel, R. M. M., G. J. J. M. van Eys, F. C. S. Ramaekers, W. J. Quax, W. T. M. Vree-Egberts, G. Schaart, H. T. M. Cuypers, and H. Bloemendal. 1987. Intermediate filament formation after transfection with modified hamster vimentin and desmin genes. *J. Cell Sci.* 88:475–482.
75. Ward, W. S., W. N. Schmidt, C. A. Schmidt, and L. S. Hnilica. 1984. Association of cytokeratin p39 with DNA in intact Novikoff hepatoma cells. *Proc. Natl. Acad. Sci. USA.* 81:419–423.
76. Weber, K., and N. Geisler. 1984. Intermediate filaments—from wool α-keratins to neurofilaments: a structural overview. *In* Cancer Cells, Vol. I. A. Levine, W. Topp, G. van de Woude, and J. D. Watson, editors. Cold Spring Harbor Laboratory, Cold Spring Harbor, NY. 153–159.
77. Wong, P. C., and D. W. Cleveland. 1990. Characterization of dominant and recessive assembly defective mutations in mouse neurofilament NF-M. *J. Cell Biol.* 111:1987–2003.